Measurement of the Induced Proton Polarization P_n in the $^{12}C(e, e'\vec{p})$ Reaction

R. J. Woo,[1,*] D. H. Barkhuff,[2,†] W. Bertozzi,[3] J. P. Chen,[4] D. Dale,[3,‡] G. Dodson,[3] K. A. Dow,[3] M. B. Epstein,[5] M. Farkhondeh,[3] J. M. Finn,[1] S. Gilad,[3] M. K. Jones,[1] K. Joo,[3,§] J. J. Kelly,[6] S. Kowalski,[3] R. W. Lourie,[2,‖] R. Madey,[7] D. J. Margaziotis,[5] P. Markowitz,[6,¶] J. I. McIntyre,[1,**] C. Mertz,[8] B. D. Milbrath,[2,††] J. Mitchell,[4] C. F. Perdrisat,[1] V. Punjabi,[9] P. M. Rutt,[10] A. J. Sarty,[3,‡‡] D. Tieger,[3] C. Tschalaer,[3] W. Turchinetz,[3] P. E. Ulmer,[11] S. P. Van Verst,[2,3,§§] C. Vellidis,[12] G. A. Warren,[3,‖‖] and L. Weinstein[11]

(Bates FPP Collaboration)

[1]*College of William and Mary, Williamsburg, Virginia 23185*
[2]*University of Virginia, Charlottesville, Virginia 22901*
[3]*Massachusetts Institute of Technology and Bates Linear Accelerator Center, Cambridge, Massachusetts 02139*
[4]*Thomas Jefferson National Accelerator Facility, Newport News, Virginia 23606*
[5]*California State University, Los Angeles, California 90032*
[6]*University of Maryland, College Park, Maryland 20742*
[7]*Kent State University, Kent, Ohio 44242*
[8]*Arizona State University, Tempe, Arizona 85287*
[9]*Norfolk State University, Norfolk, Virginia 23504*
[10]*Rutgers University, Piscataway, New Jersey 08855*
[11]*Old Dominion University, Norfolk, Virginia 23529*
[12]*University of Athens, Greece*

(Received 29 July 1997)

The first measurements of the induced proton polarization P_n for the $^{12}C(e, e'\vec{p})$ reaction are reported. The experiment was performed at quasifree kinematics for energy and momentum transfer $(\omega, q) \approx$ (294 MeV, 756 MeV/c) and sampled a missing momentum range of 0–250 MeV/c. The induced polarization arises from final-state interactions and for these kinematics is dominated by the real part of the spin-orbit optical potential. The distorted-wave impulse approximation provides good agreement with data for the $1p_{3/2}$ shell. The data for the continuum suggest that both the $1s_{1/2}$ shell and underlying $\ell > 1$ configurations contribute. [S0031-9007(97)05106-5]

PACS numbers: 24.70.+s, 24.10.Ht, 25.30.Dh, 25.30.Fj

Single-nucleon knockout by electron scattering is sensitive to both the nuclear spectral function and to the properties of the electromagnetic current in the nuclear medium; recent reviews of this subject may be found in Refs. [1–5]. Single-hole momentum distributions for discrete states of the residual nucleus are usually extracted from spin-averaged differential cross section data. Additional insight into the reaction mechanism can be obtained by separation of the unpolarized response functions. Even more discriminating tests of the reaction mechanism are provided by measurements of the polarization of the ejectile. In this Letter we report the first measurements of recoil polarization for protons ejected from a nucleus of $A > 2$ via electron scattering, specifically the $^{12}C(e, e'\vec{p})$ reaction.

Nucleon knockout reactions of the type $A(\vec{e}, e'\vec{N})B$ initiated by a longitudinally polarized electron beam and for which the ejectile polarization is detected may be described by a differential cross section of the form [6,7]

$$\frac{d\sigma_{hs}}{d\varepsilon_f d\Omega_e d\Omega_N} = \frac{\sigma_0}{2}[1 + \boldsymbol{P}\cdot\boldsymbol{\sigma} + h(A + \boldsymbol{P}'\cdot\boldsymbol{\sigma})], \tag{1}$$

where ε_f is the scattered electron energy, σ_0 is the unpolarized cross section, h is the electron helicity, s denotes the nucleon spin projection upon $\boldsymbol{\sigma}$, $\boldsymbol{P}$ is the induced polarization, A is the electron analyzing power, and $\boldsymbol{P}'$ is the polarization transfer. Each of the observables may be expressed in terms of response functions $R^s_{\alpha\beta}$ [1]. The response functions are all bilinear combinations of matrix elements of the nuclear electromagnetic current operator.

For coplanar kinematics in which the ejectile momentum lies within the electron scattering plane, $\boldsymbol{P}$ must be normal to the scattering plane while $\boldsymbol{P}'$ lies within the scattering plane. Hence, the net ejectile polarization for an unpolarized beam and coplanar kinematics is normal to the scattering plane. The polarization is calculated in the helicity basis of Ref. [1]. For this experiment performed with $\mathbf{p}'$ (the ejectile three-momentum) on the large-angle side of $\mathbf{q}$ (the three-momentum transfer), characterized by $\phi_{pq} = 180^{\circ}$, $\hat{\boldsymbol{n}}$ points vertically downwards in the laboratory.

It can be shown that P_n for the one-photon exchange approximation vanishes in the absence of final-state interactions (FSI) between the ejectile and the residual system. Within the distorted-wave impulse approximation (DWIA) FSI is usually described by an optical-model potential of the form

$$\begin{aligned} U(\mathbf{r}) &= U^C(r) + U^{LS}(r)\boldsymbol{\sigma}\cdot\boldsymbol{L}, \\ U^C(r) &= V^C(r) + iW^C(r), \\ U^{LS}(r) &= V^{LS}(r) + iW^{LS}(r), \end{aligned} \tag{2}$$

 0031-9007/98/80(3)/456(4)$15.00

where U^C and U^{LS} are complex central and spin-orbit potentials, respectively. Although the optical potential for elastic scattering from the ground state can be fit to nucleon-nucleus scattering data, no such data exist for the excited states of the residual system that are reached by knockout. Furthermore, electromagnetic knockout reactions probe the spatial distributions of these potentials differently than do elastic scattering experiments. The dynamics of FSI in the continuum may also be more complicated, requiring explicit channel coupling. Therefore, P_n provides an important independent test of the optical model, especially for final states in the continuum.

The experiment was performed at the MIT-Bates Linear Accelerator Center using an unpolarized electron beam with an energy of 579 MeV, an average current of 25 μA, and a 1% duty cycle. The carbon target had a thickness of 254 mg/cm^2. Scattered electrons and recoil protons were detected in coincidence using the MEPS and OHIPS spectrometers, respectively. Both spectrometers consist of two quadrupoles followed by a 90° vertically bending dipole (QQD) and are instrumented with vertical drift chambers for track reconstruction and scintillation detectors for timing. In addition, MEPS contains an Aerogel Čerenkov detector for pion rejection.

The proton polarization was measured in the newly commissioned focal plane polarimeter (FPP) consisting of a carbon analyzer bracketed by two pairs of multiwire proportional chambers. A fast hardware trigger system was used to reject small-angle Coulomb scattering events which have small analyzing power [8]. The analyzing power (A_y) for $120 \leq T_p \leq 200$ MeV was measured at the Indiana University Cyclotron Facility using proton beams of known polarization with this FPP [9]. These data were combined with the world's p–^{12}C A_y data for $155 \leq T_p \leq 300$ MeV and parametrized in the form introduced by Ref. [10]. For this experiment, a 9-cm thick carbon analyzer was used which provided an average A_y of 0.53. The uncertainty in the measured proton polarization due to A_y was 1.6%. Details concerning the spectrometers and the FPP can be found elsewhere [11,12].

The electron spectrometer was set at a scattering angle of 120.3° and a central momentum of 280 MeV/c. The proton spectrometer was set at a central momentum of 756 MeV/c; three angle settings (22.03°, 26.62°, and 31.00°) were used to cover the missing momentum range $0 \leq p_m \leq 250$ MeV/c. The ejectile energy for the ground state of ^{11}B was approximately constant at a central value of 274 MeV with $Q^2 = 0.5$ (GeV/c)^2. The data were combined and binned into p_m bins of 50 MeV/c ranging from 0 to 250 MeV/c. They were further separated into four missing energy (E_m) bins: A bin from 16.0 to 20.4 MeV where the data were dominated by $1p_{3/2}$ shell knockout, two bins from 28.0 to 39.0 MeV and from 39.0 to 50.0 MeV where the reaction is a mixture of $1s_{1/2}$ shell knockout and continuum effects, and a bin from 50.0 to 75.0 MeV where continuum effects dominate. The measured polarizations were corrected for accidental coincidences. The signal to noise ratio ranged from 17:1 for $1p_{3/2}$ shell knockout in the 100–150 MeV/c p_m bin to ≈1:1 for the $50 \leq E_m \leq 75$ MeV bins.

The polarization at the target is related to the polarization at the focal plane by $P_n^{\text{tgt}} = S_{nx} \cdot P_x^{fp}$ where S_{nx} is a spin-transport coefficient that includes transformations between coordinate systems, precession in the magnetic fields, and the effects of finite acceptance. For our application, $S_{nx} \approx (\cos\chi_0)^{-1}$, where $\chi_0 = 207.3°$ is the mean spin-precession angle. Small corrections for finite acceptance were made by modifying the Monte Carlo program MCEEP [13] to use the spin-transport matrices produced by COSY [14]. The net effect upon S_{nx} varies slowly with (p_m, E_m) and was found to be in the range $\pm 0.03 \pm 0.03$, where the uncertainty includes an estimate of the model dependence of the Monte Carlo simulation. The extracted transverse polarization (P_t) averaged over all bins, was $P_t = 0.008 \pm 0.018$. Also, bin by bin, P_t was consistent with zero. Instrumental false asymmetries for the P_n measurements were shown to be less than ± 0.005 from the elastic hydrogen FPP measurement [15]. Because the induced polarization of elastically scattered protons from an unpolarized electron beam is constrained to be zero in the one-photon exchange limit, any measured P_n provides a means of normalizing the FPP.

Measured polarizations for several E_m bins are compared in Fig. 1 with DWIA calculations using the effective momentum approximation; details of the DWIA formalism may be found in Refs. [1,16]. We used momentum distributions fitted to ^{12}C$(e, e'\vec{p})$ data by van der Steenhoven *et al.* [17] and the energy-dependent ^{12}C optical potential of Cooper *et al.* [18] (EDAIC). The Dirac scalar and vector potentials were transformed to equivalent Schrödinger form and the Darwin nonlocality factor was included. Figure 1 shows that DWIA calculations agree reasonably well with the P_n data for the $1p_{3/2}$ shell with a systematic underestimate of about 10%. The comparison between DWIA calculations and data for the $1s_{1/2}$ is complicated by the presence of an underlying continuum that may contain significant $\ell > 0$ contributions. The induced polarization for $28 \leq E_m \leq 39$ MeV is consistent with DWIA calculations for the $1s_{1/2}$ shell, whereas for $E_m >$ 50 MeV (Fig. 2) we find a positive P_n. This result suggests that the polarization of the continuum beneath the $1s_{1/2}$ shell, composed primarily of configurations with $\ell > 1$, is positive and tends to dilute the negative polarization expected for the $1s_{1/2}$ shell. Thus the $39 \leq E_m \leq 50$ MeV bin retains little net polarization where these opposing contributions tend to cancel. Note that this effect increases with increasing p_m.

The sensitivity to the choice of optical potential is illustrated in Fig. 1 by comparing calculations based upon the EDAIC and empirical effective interaction (EEI) optical models. The EEI model folds a density-dependent empirical effective interaction with the nuclear density. This interaction is fitted to proton-nucleus elastic and inelastic scattering data for several states of several targets

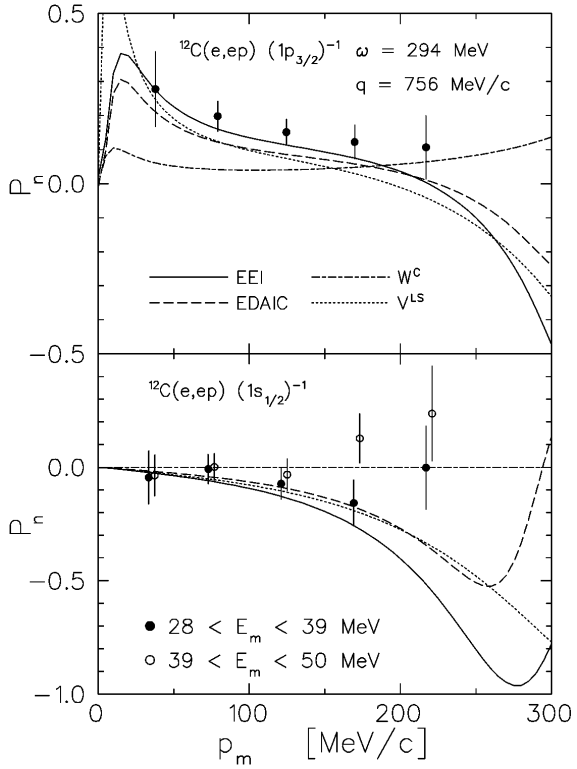

FIG. 1. Polarization for the $^{12}\mathrm{C}(e,e'\vec{p})$ reaction. Data for $E_m \leq 24$ MeV are compared with DWIA calculations for $1p_{3/2}$ knockout (top). Data for $28 \leq E_m \leq 39$ MeV and $39 \leq E_m \leq 50$ MeV (bottom) are compared with calculations for $1s_{1/2}$ knockout, although the relative importance of underlying $\ell > 0$ configurations increases with p_m and E_m. Note that a symmetric ± 2 MeV/c shift in p_m has been put in to separate the data from the two bins. The solid curves show DWIA calculations using an optical potential based upon an EEI model. The long dashed curves use the EDAIC potential, whereas other curves show the effect of individual components of the optical potential using the EDAIC potential.

simultaneously using procedures developed in Ref. [19]. However, because the nearest available energies are 200 and 318 MeV [20], a linear interpolation with respect to ejectile energy was performed. We find that the EEI model yields somewhat stronger P_n and better agreement with the data for the $1p_{3/2}$ shell.

It is also instructive to examine the contributions of various components of the optical potential separately. These are illustrated in Fig. 1 by calculations using the EDAIC potential in which all other parts of the optical potential were turned off. Of course, these separated polarizations do not simply add when the full potential is used. There are two dominant sources of P_n: the imaginary central (W^C) and real spin-orbit (V^{LS}) potentials.

The most familiar source of P_n is produced by W^C and arises from the correlation between absorption and initial spin that is commonly known as the Newns polarization [21,22] or the Maris effect [23]. However, spin-orbit distortion is the largest source of P_n for the present reaction. Although the effect of spin-orbit distortion upon ejectile polarization has been studied for $(d,\vec{p})$ reactions

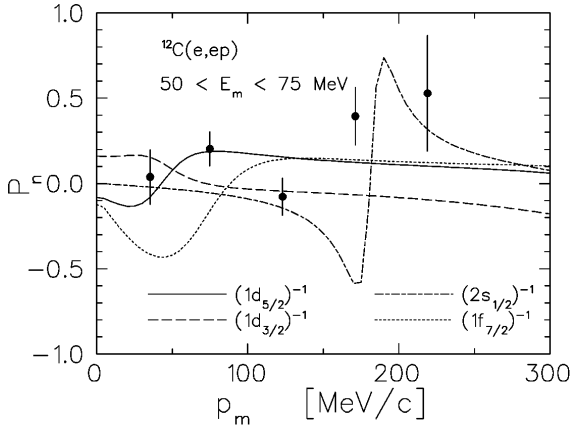

FIG. 2. Polarization for the $^{12}\mathrm{C}(e,e'\vec{p})$ reaction. Data for $50 \leq E_m \leq 75$ MeV are compared with calculations using the EDAIC potential for single-nucleon knockout from various orbitals.

at low energies [24–26], there exists little data for P_n in nucleon knockout at intermediate energies. The nature of this effect can be understood using a semiclassical argument [24] based upon the spin-orbit force:

$$F^{LS} = -\nabla[V^{LS}(r)\boldsymbol{\sigma}\cdot\boldsymbol{L}] = -\hat{\boldsymbol{r}}\,\frac{\partial V^{LS}(r)}{\partial r}\,\boldsymbol{\sigma}\cdot\boldsymbol{L} + V^{LS}(r)\boldsymbol{\sigma}\times\boldsymbol{p}'. \quad (3)$$

The first term is a central spin-orbit force which produces spin-correlated changes in the magnitude of the ejectile momentum and is most important for parallel kinematics. The second term is most effective in quasiperpendicular kinematics where spin-up (spin-down) protons are deflected toward the right (left), which for $\phi_{pq} = 180^{\circ}$ increases (decreases) the missing momentum. The polarization induced by this effect is greatest where the slope of the initial momentum distribution is largest. When $\ell > 0$ a shift of the rising slope of the momentum distribution toward larger angles for spin-up yields $P_n > 0$, whereas the falling slope of an $\ell = 0$ momentum distribution yields $P_n < 0$ for small p_m. This argument explains the sign of P_n for both the $1p_{3/2}$ and $1s_{1/2}$ states at small p_m. Furthermore, it suggests that zero crossings in the V^{LS} contribution to P_n should occur near extrema of the momentum distribution, but their precise locations depend upon more complicated geometrical and refractive effects.

In Fig. 2 we compare P_n for the deep continuum, $50 \leq E_m \leq 75$ MeV with DWIA calculations for single-nucleon knockout from several orbitals that might be populated by $2p2h$ ground-state correlations. Although the overlap functions are not necessarily those of the mean field, we used Woods-Saxon potentials with depths chosen to reproduce a central missing energy $E_m = 62$ MeV. For $p_m > 100$ MeV/c we find that knockout from the $1d_{5/2}$ or $1f_{7/2}$ orbital would produce a positive P_n. In addition, the extra node in the $2s_{1/2}$ wave function leads to a rapid sign change in its contribution to P_n in the vicinity of $p_m \sim 180$ MeV/c. Although this feature will

probably be smeared in a more realistic continuum calculation, a small admixture of this configuration could have an important effect upon P_n for the continuum at large p_m where the $1s_{1/2}$ contribution is decreasing rapidly. Therefore, although more detailed calculations are needed to properly evaluate the effect of multinucleon mechanisms both in FSI and in the absorption of the virtual photon, it appears that single-nucleon knockout from orbitals above the Fermi level that would be unpopulated in the absence of two body correlations could account for the positive P_n we observe in the deep continuum.

Summarizing, we have performed the first measurements of induced polarization for the $^{12}\mathrm{C}(e, e'\vec{p})$ reaction in quasiperpendicular kinematics for $p_m \leq 250$ MeV/c. The induced polarization is primarily sensitive to FSI and we have illustrated the roles of each component of the optical potential. For the present kinematics, the real part of the spin-orbit potential is the dominant source of P_n. The data for $1p_{3/2}$ shell are in reasonable agreement with standard DWIA calculations based upon phenomenological optical potentials fit to elastic scattering data for the ground state. Slightly better agreement with the $1p_{3/2}$ shell data is obtained using a density-dependent EEI fitted to proton-nucleus elastic and inelastic scattering data. The data for the $1s_{1/2}$ region are also consistent with DWIA calculations provided that allowance is made for the opposite polarization arising from more complicated contributions to the continuum. Improved statistical precision should allow the multipole structure of the continuum and variations of FSI for highly excited residual systems to be probed. Future experiments with polarized electron beams will measure polarization transfer observables that are expected to be sensitive to two-body currents and/or modification of the one-body electromagnetic current, but relatively insensitive to FSI. Such data, combined with precise P_n measurements, will result in considerably more stringent tests of the dynamical ingredients of the $(\vec{e}, e'\vec{N})$ process.

The authors gratefully acknowledge the work of the staff at MIT-Bates. We also thank N. S. Chant for discussions of the history of induced polarization in knockout and transfer reactions. This work was supported in part by the U.S. Department of Energy under Grants No. DE-FG05-89ER40525 and No. DE-FG05-90ER40570 and by the National Science Foundation under Grants No. PHY-89-193959, No. PHY-91-12816, No. PHY-93-11119, No. PHY-94-05315, No. PHY-94-09265, and No. PHY-94-11620. One of us (R. W. L.) acknowledges the support of an NSF Young Investigator award and a NATO Collaborative Research grant.

*Present address: U. Manitoba/TRIUMF, Vancouver, B.C. V6T 2A3.
†Present address: Massachusetts Institute of Technology, Cambridge, MA 02139.
‡Present address: University of Kentucky, Lexington, KY 40506.
§Present address: Thomas Jefferson National Accelerator Facility, Newport News, VA 23606.
‖Present address: State University of New York at Stony Brook, Stony Brook, NY 11794.
¶Present address: Florida International University, Miami, FL 33199.
**Present address: Rutgers University, Piscataway, NJ 08855.
††Present address: Eastern Kentucky University, Richmond, KY 40475.
‡‡Present address: Florida State University, Tallahassee, FL 32306.
§§Present address: Washington Department of Health, Division of Radiation Protection, Olympia, WA 98504.
‖‖Present address: Universität Basel, CH-4056 Basel, Switzerland.

[1] J. J. Kelly, Adv. Nucl. Phys. **23**, 75 (1996).
[2] S. Boffi, C. Giusti, and F. D. Pacati, Phys. Rep. **226**, 1 (1993).
[3] S. Boffi, C. Giusti, F. D. Pacati, and M. Radici, *Electromagnetic Response of Atomic Nuclei* (Oxford University Press, Oxford, 1996).
[4] A. E. L. Dieperink and P. K. A. de Witt Huberts, Ann. Rev. Nucl. Part. Sci. **40**, 239 (1990).
[5] S. Frullani and J. Mougey, in *Advances in Nuclear Physics*, edited by J. W. Negele and E. Vogt (Plenum Press, New York, 1984), Vol. 14.
[6] C. Giusti and F. D. Pacati, Nucl. Phys. **A504**, 685 (1989).
[7] A. Picklesimer and J. W. van Orden, Phys. Rev. C **40**, 290 (1989).
[8] R. W. Lourie *et al.*, Nucl. Instrum. Methods Phys. Res., Sect. A **306**, 83 (1991).
[9] R. W. Lourie *et al.*, IUCF Sci. Tech. Rept. **135** (1992–1993).
[10] E. Aprile-Giboni *et al.*, Nucl. Instrum. Methods Phys. Res. **215**, 147 (1983).
[11] J. I. McIntyre, Ph.D. thesis, College of William and Mary, 1996 (unpublished).
[12] R. J. Woo, Ph.D. thesis, College of William and Mary, 1996 (unpublished).
[13] P. E. Ulmer, TJNAF Report No. TJNAF-TN-91-101, 1991.
[14] M. Berz, Nucl. Instrum. Methods Phys. Res., Sect. A **298**, 364 (1990).
[15] B. D. Milbrath *et al.* (to be published).
[16] J. J. Kelly, Phys. Rev. C **56**, 2672 (1997).
[17] G. van der Steenhoven *et al.*, Nucl. Phys. **A480**, 547 (1988); G. van der Steenhoven *et al.*, Nucl. Phys. **A484**, 445 (1988).
[18] E. D. Cooper *et al.*, Phys. Rev. C **47**, 297 (1993).
[19] J. J. Kelly, Phys. Rev. C **39**, 2120 (1989).
[20] J. J. Kelly and S. J. Wallace, Phys. Rev. C **49**, 1315 (1994).
[21] H. C. Newns, Proc. Phys. Soc. London Sect. A **66**, 477 (1953).
[22] H. C. Newns and M. Y. Refai, Proc. Phys. Soc. London Sect. A **71**, 627 (1958).
[23] G. Jacob *et al.*, Nucl. Phys. **A257**, 517 (1976).
[24] S. T. Butler, in *Proceedings of the Rutherford Jubilee International Conference*, edited by J. B. Birks (Heywood and Company, London, 1961), p. 492; L. J. B. Goldfarb *ibid.*, p. 479.
[25] D. Robson, Nucl. Phys. **22**, 34 (1961).
[26] R. C. Johnson, Nucl. Phys. **35**, 654 (1962).